

Transiting exoplanets from the *CoRoT* space mission[★]

XV. CoRoT-15b: the link between massive exoplanets and low-mass stars

Bouchy, F.^{5,6}, Deleuil, M.³, Guillot, T.¹³, Aigrain, S.¹, Carone, L.¹⁷, Cochran, W.D.²⁰, Csizmadia, Sz.⁹, Almenara, J.M.^{7,21}, Alonso, R.¹⁸, Auvergne, M.², Baglin, A.², Barge, P.³, Bordé, P.⁴, Deeg, H.J.^{7,21}, Díaz, R.F.⁶, Dvorak, R.⁸, Endl, M.²⁰, Erikson, A.⁹, Ferraz-Melo, S.¹⁰, Fridlund, M.¹¹, Gazzano, J.C.³, Gillon, M.¹², Hatzes, A.¹⁴, Havel, M.¹³, Hébrard, G.⁶, Jorda, L.³, Léger, A.⁴, Lovis, C.¹⁸, Llebaria, A.³, Lammer, H.¹⁵, Mazeh, T.¹⁶, Moutou, C.³, Ollivier, M.⁴, Parvaianen, H.^{7,21}, Pätzold, M.¹⁷, Queloz, D.¹⁸, Rauer, H.⁹, Rouan, D.¹, Santerne, A.³, Schneider, J.¹⁹, Tingley, B.^{7,21}, and Wuchterl, G.¹⁴

(Affiliations can be found after the references)

Received ; accepted

ABSTRACT

We report the discovery by the *CoRoT* space mission of a transiting brown dwarf orbiting a F7V star in 3.06 days. CoRoT-15b, with a radius of $1.22 \pm 0.07 R_{\text{Jup}}$ and a mass of $64 \pm 5 M_{\text{Jup}}$, is the second transiting companion lying in the theoretical mass domain of brown dwarfs.

Key words. brown dwarfs - planetary systems - low-mass - techniques: photometry - techniques: radial velocities - techniques: spectroscopic

1. Introduction

The space *CoRoT* mission (Baglin et al. 2009), in operation since start of 2007 and extended to end of 2013, is design to find transiting exoplanets. A natural product of this mission is that any object with size of Jupiter or lower that transits its host star can be detected. This includes stellar and sub-stellar companions such as M-dwarfs and brown dwarfs (BDs). In the mass-radius diagram, there is up to day only one known brown-dwarf, CoRoT-3b (Deleuil, et al. 2008), located in the gap in mass between planetary and low-mass star companions. Determination of the physical properties of such objects are fundamental to understand the link between the population of planets and low-mass stars and to distinguish the formation and evolution processes of the two populations.

We report in this paper the discovery of a new transiting brown-dwarf by *CoRoT* established and characterized thank to ground-based follow-up observations. CoRoT-15b, with an estimated radius of $1.22 R_{\text{Jup}}$ and an estimated mass of $64 M_{\text{Jup}}$, orbits in 3.06 days an F-type dwarf with solar metallicity.

2. *CoRoT* observations

SRa02 was the seventh field observed with *CoRoT* in the second year after its launch. It corresponds to the third short run and was located towards the so-called galactic anti-center direction. This run started on 2008 October 11 and ended on 2008 November 12, constituting of a total of 31.7 days of almost-continuous observations.

More than 30 multi-transiting candidates for planets were identified among the 10265 targets of the SRa02 field. About half of them were clearly identified as binaries from light-curve analysis and a tenth of high priority planetary candidates were selected in this short run including SRa02_E1_4106 afterwards called CoRoT-15. The various ID of this target, including coordinates and magnitudes are listed in table 1.

Table 1. IDs, coordinates and magnitudes.

<i>CoRoT</i> window ID	SRa02_E1_4106
<i>CoRoT</i> ID	221686194
USNO-B1 ID	0961-0097866
2MASS ID	06282781+0611105
RA (J2000)	06:28:27.82
Dec (J2000)	+06:11:10.47
B1 ^a	16.85
B2 ^a	16.59
R1 ^a	15.47
R2 ^a	15.43
I ^a	14.83
J ^b	13.801 ± 0.026
H ^b	13.423 ± 0.037
K ^b	13.389 ± 0.050

^a from USNO-B1 catalog

^b from 2MASS catalog

3. *CoRoT* light curve analysis

CoRoT-15, with an estimated V magnitude close to 16, is located at the faint end of the stellar population observed by *CoRoT*. In this magnitude domain, the signal is not sufficient to split the photometric aperture in three colors and the ex-

[★] The *CoRoT* space mission, launched on December 27th 2006, has been developed and is operated by CNES, with the contribution of Austria, Belgium, Brazil, ESA (RSSD and Science Programme), Germany and Spain. Observations made with HARPS spectrograph at ESO La Silla Observatory (184.C-0639).

tracted lightcurve, also called white lightcurve, is monochromatic (Lebaria & Guterman 2006). The sampling rate was at 512 seconds during the whole run and not oversampled to 32 seconds since this candidate was not identified with the alarm mode (Surace et al. 2008). Fig. 1 shows the lightcurve of CoRoT-15 delivered by the N2 data levels pipeline. This lightcurve is quite noisy and is affected by several cosmic ray events as well as possible stellar variability.

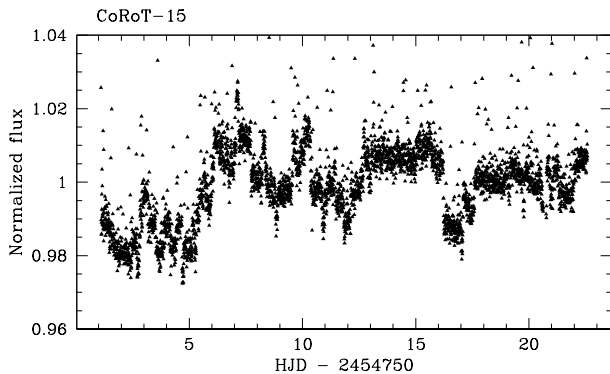


Fig. 1. Raw Light Curve of CoRoT-15.

A first analysis of the lightcurve, based on fit of each individual transits by a trapezoidal, reveals periodic transits with depth of 0.68% and a period of 3.0608 ± 0.0008 days. Out-of-transit points within the small environment (± 3 times the duration) of each individual transits were selected, and adjusted separately by a parabola. A sigma-clipping was applied in order to exclude all out-of-transit points far from the parabola (5σ clip). Each transit observations (both in-transit-points and out-of-transit points) were divided by the adjusted parabola in order to filter the light curve. Although the light curve was obtained in the 512 seconds sampling rate, we applied a bin-averaging to increase the signal-to-noise ratio. Uncertainties of the individual points were estimated from the standard deviation of the points in the bin. The whole corrected lightcurve folded at the period of 3.06 days is shown in Fig. 2. The dispersion of the residuals is 2 mmag.

Since the *CoRoT* lightcurve is relatively noisy, no meaningful limits to either the visible-light albedo of the companion nor to its dayside surface temperature could be established.

From the raw lightcurve, we tried to estimate the stellar rotation period. We filtered out variations with timescales shorter than 15 data points (~ 2.13 h) to reduce sensitivity to the satellite orbital effects so on, then we removed the transits. The computed LS periodogram appears to be quite noisy and affected by low-level discontinuities in the lightcurve. There is tentative evidence of a possible rotational modulation at either 2.9 or 6.3 days in the light curve, but the data does not enable us to estimate the period more precisely or to distinguish between these two values.

4. Ground-based observations

4.1. Ground-based Photometric follow-up

Ground-based photometry is performed with the aim to refine the target ephemeris, to verify that none of its closest contaminant stars correspond to an eclipsing binary and to determine the contamination from nearby stars inside *CoRoT*'s photometric aperture mask (Deeg et al. 2009). CoRoT-15 was observed during a transit event on 2010 January 13 with time-series pho-

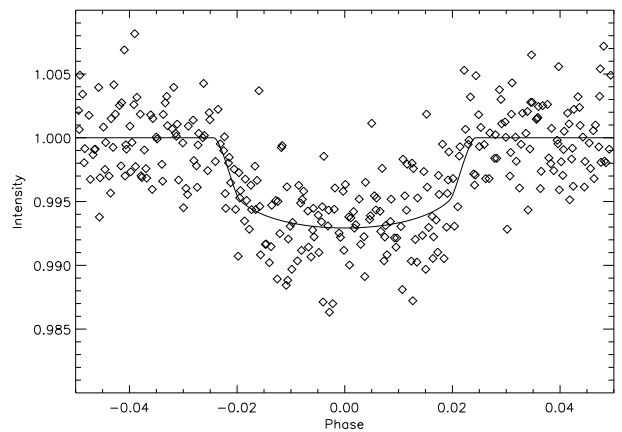


Fig. 2. Phase-folded Light Curve of CoRoT-15 with period of 3.0608 days superimposed with the transit fit.

tometry at the IAC80 telescope, from HJD 2455209.480 to .676. The resultant lightcurve was not sufficiently precise to identify the expected transit on the target, due to photometric errors introduced from a thin cirrus coverage. However, the absence of large brightness variations in the neighboring stars allowed to exclude nearby eclipsing binaries as a source of the signals that were observed by *CoRoT*. The contamination factor was derived from a measure of the distance and brightness of the nearby stars on a subset of these IAC80 R-filter images obtained with the best seeing of that night (1.7 arcsec). Ten nearby stars were identified, with 6 of them contaminate the *CoRoT* window aperture with flux level amount of $1.9 \pm 0.3\%$ of the main target flux. We checked furthermore that none of the known nearby stars is bright enough to be a contaminant eclipsing binaries. The image of the sky around CoRoT-15 is shown in Fig. 3.

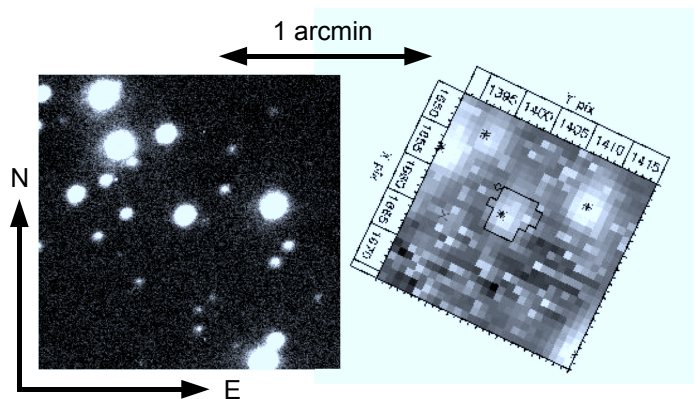


Fig. 3. The image of the sky around CoRoT-15 (star in the centre). Left: R-filter image with a resolution of $1.7''$ taken with the IAC80 telescope. Right: Image taken by *CoRoT*, at the same scale and orientation. The jagged outline in its centre is the photometric aperture mask; indicated are also *CoRoT*'s x and y image coordinates and positions of nearby stars which are in the Exo-Dat (Deleuil et al 2009) database.

4.2. Radial velocity follow-up

Radial velocity (RV) observations of CoRoT-15 were performed with the HARPS spectrograph (Mayor et al. 2003) based on the 3.6-m ESO telescope (Chile) as part of the ESO large program 184.C-0639 and with the HIRES spectrograph (Vogt et al. 1994)

Table 2. Radial velocity measurements of CoRoT-15 obtained by HARPS and HIRES. BJD is the Barycentric Julian Date.

BJD	RV	$\pm 1 \sigma$
	[km s ⁻¹]	[km s ⁻¹]
HARPS 3.6-m ESO		
55159.81312	9.944	0.308
55169.77922	2.107	0.315
55235.60498	2.849	0.380
55236.59903	8.057	0.392
55241.55686	0.119	0.338
55243.55544	-2.422	0.222
55246.56091	-2.684	0.434
55247.55392	-1.318	0.411
55248.54372	10.235	0.357
HIRES 10-m Keck		
55221.76973	1.084	0.291
55221.81404	0.890	0.189
55221.82490	0.556	0.289
55221.89482	-0.232	0.220
55221.90689	-0.492	0.216
55221.97788	-1.869	0.353
55221.99025	-1.750	0.147
55222.98656	-3.193	0.340
55222.99752	-3.587	0.226
55223.73904	6.527	0.113
55224.82036	1.593	0.374
55224.83152	1.818	0.303
55225.04022	-1.345	0.515

based on the 10-m Keck-1 telescope as part of NASA’s key science project to support the *CoRoT* mission.

HARPS was used with the observing mode obj_AB, without simultaneous thorium in order to monitor the Moon background light on the second fiber. The exposure time was set to 1 hour. A set of 9 spectra was recorded between November 24th 2009 and February 21th 2010. We reduced HARPS data with the pipeline based on the cross-correlation techniques (Baranne et al. 1996; Pepe et al. 2002). The signal-to-noise ratio (SNR) per pixel at 550 nm is in the range 3 to 7.8 for this faint target. It corresponds to the faint end in magnitude for HARPS follow-up observations. Radial velocities were obtained by weighted cross-correlation with a numerical G2 mask.

HIRES observations were performed with the red cross-disperser and the I₂-cell to measure RVs. We used the 0.861” wide slit that leads to a resolving power of $R \approx 50,000$. The contamination of the HIRES spectra by scattered moon light was significant for this faint target, but the 7” tall decker allowed us to properly correct for the background light. Over a 4-night run from 2010 January 25 to January 28 we have collected 13 spectra of CoRoT-15 with the I₂-cell, and three spectra without the cell. These 3 spectra were co-added to serve as stellar template for the RV measurements, and to be used for the determination of stellar parameters (see Sect. 4.3). The average SNR of the spectra with the I₂-cell range from 13 to 22 (per pixel) in the iodine region from 500–620nm. Differential radial velocities were computed using our *Austral* Doppler code (Endl et al. 2000). Nine RV measurements were made during a transit event on 2010 January 25 but were not enough sensitive to detect the signature of the Rossiter-McLaughlin effect expected to have, for this high rotating star, an amplitude of about 100 m s⁻¹.

The HARPS and HIRES radial velocities are given in Table 2. The two sets of relative radial velocities were simultaneously fitted with a Keplerian model, with the epoch and period of the transit being fixed at the *CoRoT* value and with an

adjusted offset between the two different instruments. No significant eccentricity was found and we decided to set it to zero. We found a systematic shift in phase using the *CoRoT* period of $P=3.0608$ days. It comes from the fact that the quite large uncertainty on the *CoRoT* period (69 seconds) may introduce 1 year after a systematic shift of more than 2 hours. We then decided to adjust the period with the RVs fixing the transit epoch as determined from *CoRoT* lightcurve $T_t=54753.5570 \pm 0.0028$. The best solution is obtained for $P=3.06039 \pm 0.00014$ days, a semi-amplitude $K=7.376 \pm 0.090$ km s⁻¹ and an RV offset 1.17 ± 0.55 km s⁻¹. The dispersion of the residuals is 0.325 km s⁻¹ and the reduced χ^2 is 0.90.

Figure 4 shows all the radial velocity measurement after subtracting the RV offset and phase folded to the updated orbital period.

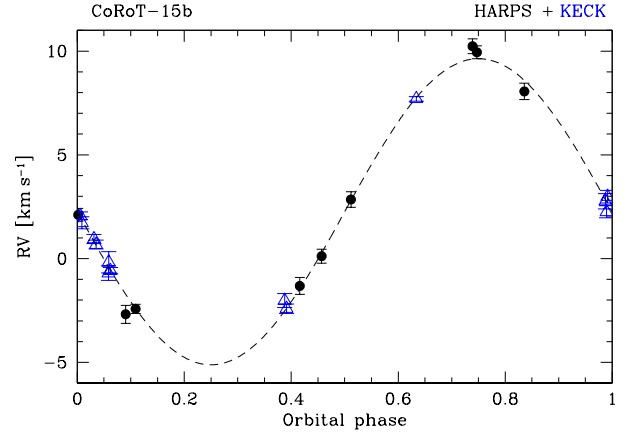


Fig. 4. Phase-folded radial velocity measurements of CoRoT-15 with HARPS (dark circle) and HIRES (open triangle)

4.3. spectral classification

Three HIRES spectra of CoRoT-15 were acquired without the iodine cell. Each spectrum was set in the heliocentric rest frame, cleaned from cosmic rays and from the moon reflected light. The co-addition of these 3 spectra results in a master spectrum covering the wavelength range from 4100 Å to 7800 Å with a SNR per element of resolution in the continuum ranging from 20 at 5300 Å up to 70 at 6820 Å. The 9 co-added HARPS spectra did not permit to reach a better SNR.

From the analysis of a set of isolated lines, we derived a $v \sin i$ of 19 ± 2 km s⁻¹. The spectroscopic analysis was carried out using the same methodology as for the previous *CoRoT* planets and described in details in Bruntt et al. (2010). However, the moderate SNR of the master spectrum of this faint target, combined to the marked rotational broadening of the spectral lines prevent us from an accurate measure of the star’s photospheric parameters. The derived stellar parameters are reported in Table 3.

Calculations using CESAM (Morel & Lebreton 2008, see also Guillot & Havel 2010) confirm these solutions, and also yield possible pre-main sequence solutions with extremely young ages, between 10 and 15 Myr. It is to note that although to 1σ of the measured T_{eff} and $M_{\star}^{1/3}/R_{\star}$ the age constraint is reasonably strong, within 3σ , any age becomes possible.

Following Santos et al. (2002) methodology, we also estimated the $v \sin i$ and the $[Fe/H]$ index from the HARPS cross-correlation average parameters (FWHM and surface). Assuming a $B - V$ of 0.5, we estimated the $v \sin i$ of the target to be $16 \pm 1 \text{ km s}^{-1}$ and a $[Fe/H]$ index close to zero (solar metallicity) in agreement with the spectral analysis.

5. System parameters

For the fit of the phase-folded corrected lightcurve, we used the equations of Mandel & Agol (2002) model assuming a circular orbit. We took into account that the contamination factor analysis from Sect. 4.1 yielded that $98.1 \pm 0.3\%$ of all the observed flux comes from the main target. The free parameters were the semi-major axis - stellar radius ratio (a/R_*), the companion-to-stellar radius ratio (R_c/R_*), the impact parameter ($b = a \cos i/R_*$, where i is the inclination) and the two limb darkening coefficients $u+ = u_a + u_b$, $u- = u_a - u_b$ (using the quadratic limb darkening law). From the stellar parameters (T_{eff} , $\log g$ and $[Fe/H]$) we fixed the limb darkening coefficient $u- = 0.38$ based on Sing et al. (2010) tables and adjusted $u+$. To find the best fit we used the recently developed Harmony Search algorithm (Geem et al. 2001) which is a genetic algorithm-type optimization method. Uncertainty on the contamination factor was propagated into the final parameters. The 1σ errors were estimated from the width of parameter distribution between χ_{min}^2 and $\chi_{\text{min}}^2 + 1$. The results are reported in Table 3.

We used the photospheric parameters from spectral analysis and the stellar density derived from the transit modeling to determine the star's fundamental parameters in the (T_{eff} , $M_*^{1/3}/R_*$) space. Using *STAREVOL* evolution tracks (Palacios, *private com.*), we find the stellar mass to be $M_* = 1.35 \pm 0.12 M_\odot$ and the stellar radius $R_* = 1.58 \pm 0.08 R_\odot$, with an age in the range 1.1–5.9 Gyr. This infers a surface gravity of $\log g = 4.17 \pm 0.15$, in good agreement with the spectroscopic value.

We derived for the transiting companion $M_c = 64 \pm 5 M_{\text{Jup}}$ and $R_c = 1.22 \pm 0.07 R_{\text{Jup}}$.

6. Discussion and Conclusion

After CoRoT-3b (Deleuil et al. 2008), CoRoT-15b is the second transiting companion that lies in the theoretical mass domain of "brown dwarfs" (13–75 M_{Jup} , if one adopts the present IAU convention). Expanding a bit the mass domain, one can easily include in this ensemble the high mass "planets" ($M \geq 10 M_{\text{Jup}}$) XO-3b (Johns-Krull et al. 2007) and WASP-18b (Hellier et al. 2009), and in the M-dwarf regime, OGLE-TR-122b (Pont et al. 2005) -123b (Pont et al. 2006) -106b (Pont et al. 2005), and HAT-TR-205-013 (Beatty et al. 2007). Interestingly, all these objects are found to orbit F-type stars, with one exception: OGLE-TR-122b orbits a G-type dwarf but has a much longer orbital period (7.3 days compared to less than 4.3 days for all other objects). F-type dwarfs have the particularity of being fast rotators, independently of their age (Nordstrom et al. 1997), a consequence of a small or inexistent outer convective zone, weak stellar winds, and reduced losses of angular momentum. We thus propose that the presence of close-in massive planets, brown dwarfs or M-dwarfs is possible around F-type stars because a faster rotation of the parent star yields an outward torque on the companion. On the contrary, G-type stars rapidly lose their angular momentum due to winds and always end up rotating more slowly than their close-in companion. The tides raised by massive compan-

Table 3. Star and companion parameters.

Parameters	Value
Transit epoch T_{tr} [HJD]	2454753.5574 \pm 0.0028
Orbital period P [days]	3.06039 \pm 0.00014
Transit duration d_{tr} [h]	3.69 \pm ??
Orbital eccentricity e	0 (fixed)
Semi-amplitude K [km s $^{-1}$]	7.376 \pm 0.090
Systemic velocity V_0 [km s $^{-1}$]	2.257 \pm 0.048
Radius ratio R_c/R_*	0.0791 \pm 0.0007
Scaled semi-major axis a/R_*	6.28 \pm 0.12
limb darkening coefficient $u+$	0.62 \pm 0.06
limb darkening coefficient $u-$ ^a	0.38 (fixed)
Impact parameter b	0.504 \pm 0.029
$M_*^{1/3}/R_*$ [solar units]	0.71 \pm 0.03
Stellar density ρ_* [$g \text{ cm}^{-3}$]	500 \pm 30
Inclination i [deg]	85.4 \pm 0.54
Effective temperature T_{eff} [K]	6350 \pm 200
Surface gravity $\log g$ [dex]	4.3 \pm 0.2
Metallicity [Fe/H] [dex]	0.1 \pm 0.2
Rotational velocity $v \sin i$ [km s $^{-1}$]	19 \pm 2
Spectral type	F7V
Star mass [M_\odot]	1.35 \pm 0.12
Star radius [R_\odot]	1.58 \pm 0.08
Distance of the system	1270 \pm 300
Age of the star [Gyr]	1.1–5.9
Orbital semi-major axis a [AU]	0.046 \pm 0.003
Companion mass M_c [M_J] ^a	64 \pm 5
Companion radius R_c [R_J] ^a	1.22 \pm 0.07
Companion density ρ_c [$g \text{ cm}^{-3}$]	46 \pm 12

^a based on tables from Sing 2010.

ions rapidly bring them into the central star (e.g. Levrard et al. 2009).

It is interesting to see that given the $v \sin i$ and stellar radius determinations, the projected spin period of the central star is $P/\sin i_* = 4.2 \pm 0.5$ days. The LS periodogram analysis of the CoRoT-15 lightcurve yields two dominant periods: one close to 6.3 days, which cannot be the star's spin period, and one close to 2.9 days. If taken as the stellar spin period, this would imply that the system is indeed stable (at least as long as the central star does not brake too much), the companion being pushed outwards.

CoRoT-15b is also extremely interesting for its size in comparison with other objects in this mass range, and of evolution tracks for hydrogen-helium brown dwarfs and stars. Figure 5 shows that it is extremely inflated compared to standard evolution tracks for these kind of objects (Baraffe et al. 2003). This is also the case of OGLE-TR-123b, OGLE-TR-106b and, but to a lesser extent, HAT-TR-205-013. In order to examine possible solutions to this puzzle, we calculate evolution tracks using CEPAM (Guillot & Morel 1995), but adding the dominant thermonuclear reaction cycle, namely the pp-chain (see Burrows & Liebert 1993). The atmospheric boundary condition is adjusted to the Baraffe et al. (2003) evolution tracks, using the analytical solution of Guillot (2010), and values of the thermal and visible mean opacities, $\kappa_{\text{th}} = 0.04 \text{ cm}^2 \text{ g}^{-1}$ and $\kappa_{\text{v}} = 0.024 \text{ cm}^2 \text{ g}^{-1}$. The model shows that irradiation effects, although quite significant for Jupiter-like planets have rather small consequences in the brown dwarf regime, and become completely negligible in

the stellar regime. We also test the possibility that these inflated sizes may be explained by the presence of cold spots on the brown dwarf, similarly to a mechanism proposed to explain that M-type star in close-in binaries also appear inflated (Chabrier et al. 2007). As shown in Fig. 5, this mechanism works only in combination with a young age for the system, and with a rather large fraction (50%) of the photosphere covered with spots. An alternative possibility is that irradiated atmospheres are much more opaque than usually thought, possibly a consequence of photochemistry and disequilibrium chemistry.

In any case, this shows that CoRoT-15b is a crucial object to understand both the dynamical and physical evolution of giant planets, brown-dwarfs and low-mass stars. Further observations aiming at obtaining more accurate spectra of the star would be highly desirable. Although this is a challenging measurement given the faintness of the target, measurement of secondary transits in the infrared would be extremely interesting because they would inform us on this rare heavily irradiated brown dwarf atmosphere.

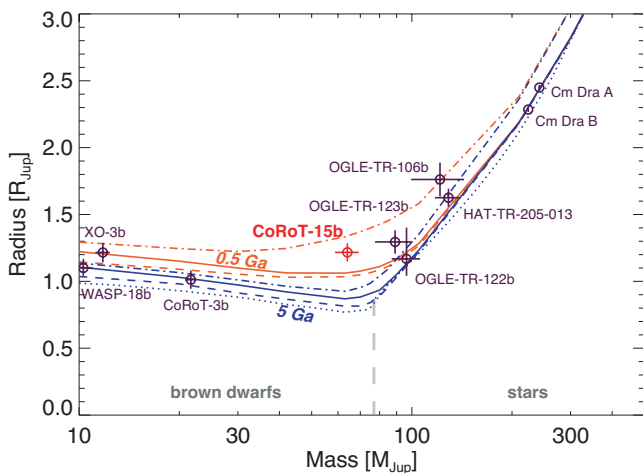


Fig. 5. Masses and radii of eclipsing brown-dwarfs and low-mass stars (circles with error bars, as labeled) compared to theoretical mass-radius relations (lines). The lines correspond to cooling ages of 0.5 (upper orange lines) and 5 Ga (lower blue lines), respectively. The dashed lines are calculated for isolated brown-dwarfs and low-mass stars. The plain lines include the effect of irradiation with $T_{\text{eq}} = 1800$ K. The dash-dotted lines include irradiation and account for a 50% coverage of the photosphere with low-temperature spots (see text). A 5 Ga isochrone for isolated brown dwarfs/M stars from Baraffe et al. (2003) is shown for comparison (dotted line).

Acknowledgements. The authors wish to thank the staff at ESO La Silla Observatory for their support and for their contribution to the success of the HARPS project and operation. The French team wish to thank the Programme National de Planétologie (PNP) of CNRS/INSU and the French National Research Agency (ANR-08-JCJC-0102-01) for their continuous support to our planet search. The team at IAC acknowledges support by grant ESP2007-65480-C02-02 of the Spanish Ministerio de Ciencia e Innovación. HIRES data presented herein were obtained at the W.M. Keck Observatory from telescope time allocated to the NASA through the agency's scientific partnership with the California Institute of Technology and the University of California.

References

Baglin A., Auvergne M., Barge P., et al., 2009, *Transiting Planets*, Proceedings of the International Astronomical Union, IAU Symposium, 253, 71
 Baraffe, I.; Chabrier, G.; Barman, T.S., et al., 2003, *A&A*, 402, 701
 Baranne, A., Queloz, D., Mayor, M., et al. 1994, *A&AS*, 119, 373

Beatty et al. 2007, *ApJ*, 663, 573
 Bruntt et al., 2010
 Burrows & Liebert 1993, *RvMP*, 65, 301
 Chabrier et al. 2007, *A&A*, 472, 17
 Deeg, H., et al., 2009 *A&A* 506 343
 Deleuil, M., Deeg, H., Alonso, R., et al., 2008, *A&A*, 491, 889
 Endl, M., Kürster, M., Els, S., 2000, *A&A*, 362, 585
 Geem, Z. W., Kim, J. H., Loganathan, G. V. 2001, *Simulation Vol. 76*, pp.60-68
 Guillot & Morel 1995, *A&A*, 109, 109
 Guillot 2010, submitted to *A&A*.
 Guillot & Havel 2010, *A&A*, submitted
 Hellier et al. 2009, *Nature*, 460, 1098
 Johns-Krull et al. 2007, *ApJ*, 677, 657
 Levrard et al. 2009, *ApJ*, 692, L9
 Llebaria, A., & Guterman, P., 2006, in *ESA Special Publication*, 1306, 293
 Mandel, K., Agol, E. 2002, *ApJ* 580, 171
 Mayor, M., Pepe, F., Queloz, D., et al. 2003, *The Messenger*, 114, 20
 Morel & Lebreton, 2008, *Ap&SS*, 316, 61
 Nordstrom, B., Stefanik, R.P., Latham, D.W., et al., 1997, *A&ASS*, 126, 21
 Pepe, F., Mayor, M., Galland, F., et al., 2002, *A&A*, 388, 632
 Pont et al. 2005, *A&A*, 433, 21
 Pont et al. 2005, *A&A*, 438, 1123
 Pont et al. 2006, *A&A*, 447, 1035
 Santos, N.C., Mayor, M., Naef, D., et al., 2002, *A&A*, 392, 215
 Sing, D., 2010, *A&A*, ...
 Surace, C., Alonso, R., Barge, P., et al., 2008, *SPIE Conf. Series*, 7019, 111
 Vogt, S.S., Allen, S.L., Bigelow, B.C., et al. 1994, *SPIE*, 2198, 362

- 1 Department of Physics, Denys Wilkinson Building Keble Road, Oxford, OX1 3RH
- 2 LESIA, Obs de Paris, Place J. Janssen, 92195 Meudon cedex, France
- 3 Laboratoire d'Astrophysique de Marseille, 38 rue Frédéric Joliot-Curie, 13388 Marseille cedex 13, France
- 4 Institut d'Astrophysique Spatiale, Université Paris XI, F-91405 Orsay, France
- 5 Observatoire de Haute Provence, 04670 Saint Michel l'Observatoire, France
- 6 Institut d'Astrophysique de Paris, 98bis boulevard Arago, 75014 Paris, France
- 7 Instituto de Astrofísica de Canarias, E-38205 La Laguna, Tenerife, Spain
- 8 University of Vienna, Institute of Astronomy, Türkenschanzstr. 17, A-1180 Vienna, Austria
- 9 Institute of Planetary Research, German Aerospace Center, Rutherfordstrasse 2, 12489 Berlin, Germany
- 10 Observatório Nacional, Rio de Janeiro, RJ, Brazil
- 11 Research and Scientific Support Department, ESTEC/ESA, PO Box 299, 2200 AG Noordwijk, The Netherlands
- 12 University of Liège, Allée du 6 août 17, Sart Tilman, Liège 1, Belgium
- 13 Thüringer Landessternwarte, Sternwarte 5, Tautenburg 5, D-07778 Tautenburg, Germany
- 14 Space Research Institute, Austrian Academy of Science, Schmiedlstr. 6, A-8042 Graz, Austria
- 15 School of Physics and Astronomy, Raymond and Beverly Sackler Faculty of Exact Sciences, Tel Aviv University, Tel Aviv, Israel
- 16 Observatoire de l'Université de Genève, 51 chemin des Maillettes, 1290 Sauverny, Switzerland
- 17 Rheinisches Institut für Umweltforschung an der Universität zu Köln, Aachener Strasse 209, 50931, Germany
- 18 Université de Nice-Sophia Antipolis, CNRS UMR 6202, Observatoire de la Côte d'Azur, BP 4229, 06304 Nice Cedex 4, France
- 19 LUTH, Observatoire de Paris, CNRS, Université Paris Diderot; 5 place Jules Janssen, 92195 Meudon, France
- 20 McDonald Observatory, The University of Texas at Austin, Austin, TX 78731, USA
- 21 Departamento de Astrofísica, Universidad de La Laguna, E-38200 La Laguna, Tenerife, Spain